0090-9556/10/3810-1714–1722$20.00
DRUG METABOLISM AND DISPOSITION
Vol. 38, No. 10
33795/3624836
DMD 38:1714–1722, 2010
Printed in U.S.A.

Metabolism of Dicentrine: Identification of the Phase I and Phase II Metabolites in Miniature Pig Urine[S]

Yi-Chun Lai, Tzong-Fu Kuo, Chien-Kuang Chen, Han-Ju Tsai, and Shoei-Sheng Lee

School of Pharmacy, College of Medicine (Y.-C.L., C.-K.C., S.-S.L.), Department and Graduate Institute of Veterinary Medicine (T.-F.K.), and Veterinary Hospital (H.-J.T.), National Taiwan University, Taipei, Taiwan, Republic of China

Received April 4, 2010; accepted July 9, 2010

ABSTRACT:

The metabolic profile of dicentrine, a selective α_1-adrenoceptor antagonist with potent antiarrhythmic and antihypertensive activities, in miniature pig urine via oral administration was investigated for the first time. The urine, collected after a single oral administration of dicentrine, was pretreated using solvent extraction and column chromatographic methods to identify the metabolites containing fractions. Twenty-four metabolites (MI-1–9 and MII-1-15), of which 21 compounds are new, were identified by mass spectrometry and high-performance liquid chromatography-diode array detector solid-phase extraction-NMR techniques. Of these, 14 metabolites (MI-5, MII-1 and 2, and MII-5-15) were further isolated for structure confirmation. The phase I metabolic transformations of dicentrine were found to be *N*-demethylation, *N*-oxidation, *O*-demethylation (9,10-OMe), *O*,*O*-demethylenation (1-OC*H*$_2$O-2), and hydroxylation at the benzylic (C-4) and the aromatic (C-3) positions, whereas those for the phase II were *O*-glucuronidation and *O*-glucosylation of the phenolic group of the phase I metabolites.

Introduction

(+)-Dicentrine, an aporphine alkaloid present abundantly in a variety of genera in the plant families Lauraceae (Chen et al., 1991), Papaveraceae (Lalezari et al., 1976), Menispermaceae (De Wet et al., 2007), and Fumariaceae (Israilov et al., 1984), was demonstrated to be a selective α_1-adrenoceptor antagonist (Teng et al., 1991) and to possess potent biological activities, including antiarrhythmic (Su et al., 1994), antiplatelet aggregation (Teng et al., 1991; Yu et al., 1992a), antihypertensive (Yu et al., 1992b), antihyperlipidemic (Yu et al., 1993), and antitumor (Stévigny et al., 2005) activities. The antiarrhythmic effect of dicentrine has been shown in rabbit (Young et al., 1994) and dog (Chang et al., 1995) models. These results showed that dicentrine was a promising drug candidate as a class I and class III antiarrhythmic agent. Another study revealed that dicentrine could relieve bladder outlet obstruction caused by benign prostatic hyperplasia (Yu et al., 1994). Oral administration of dicentrine (5 mg/kg) to conscious spontaneously hypertensive rats resulted in a significant reduction in mean arterial pressure, which was observed 1 h after administration, and the hypotensive effect persisted for more than 15 h (Yu et al., 1992b). This long-acting phenomenon indicated that dicentrine had either a long half-life or active metabolites. One pharmacokinetic study of dicentrine (10 mg/kg i.v.) in rat (Tsai et al., 1996) revealed that the distribution and elimination of dicentrine were extremely fast [$t_{1/2\alpha}$ 4.32 min, $t_{1/2\beta}$ 45.20 min, and clearance 0.51 l/(kg · min)], indicating that dicentrine was easily metabolized. Thus, the long-acting effect should arise from the active metabolites. However, dicentrine metabolites have not been reported yet. Therefore, we investigated the metabolites in the urine of miniature pigs after intragastric oral administration of dicentrine mesylate.

Because the amounts of metabolites are usually minute, their structures are commonly analyzed by liquid chromatography-MS/MS. However, the information provided by this technique is usually not enough to determine the exact structure. Up to now, NMR and HPLC were recognized generally to be the most powerful tools for structure elucidation and analytic scale separation, respectively. Hence, the HPLC-NMR technique has been applied to study the metabolic profile of some drugs (Burton et al., 1997; Spraul et al., 2003). The HPLC-SPE-NMR technique has also been successfully applied in analysis of natural products (Wang and Lee, 2005; Lam et al., 2007; Lee et al., 2007) as well as in identification of certain metabolites (Godejohann et al., 2004; Sandvoss et al., 2005). In the present study, HPLC-SPE-NMR, along with HPLC-HRESIMS, was applied to the characterization of the dicentrine metabolites in the urine of miniature pigs. The structures of major metabolites were confirmed by spectral analysis through further isolation.

This study was supported by the National Science Council, Republic of China [Grants NSC96-2323-B-002-001, NSC97-2323-B-002-001].

Article, publication date, and citation information can be found at http://dmd.aspetjournals.org.

doi:10.1124/dmd.110.033795.

[S] The online version of this article (available at http://dmd.aspetjournals.org) contains supplemental material.

ABBREVIATIONS: MS/MS, tandem mass spectrometry; HPLC, high-performance liquid chromatography; SPE, solid-phase extraction; HRESIMS, high-resolution electrospray ionization mass spectrometry; MeOH, methanol; MS, mass spectrometry; 2D, two dimensional; HMQC, heteronuclear multiple quantum correlation; HSQC, heteronuclear single quantum correlation; HMBC, heteronuclear multiple bond coherence; NOE, nuclear Overhauser effect; NOESY, nuclear Overhauser effect spectroscopy; DAD, diode array detector; RP, reverse-phase; TFA, trifluoroacetic acid; ESI, electrospray ionization; 1D, one-dimensional; GlcUA, glucuronyl.

Materials and Methods

Materials and Supplies. HPLC-pure dicentrine (**1**) was provided by Dr. Chien-Chih Chen, National Research Institute of Chinese Medicine, Taipei, Republic of China. Its mesylate salt, m.p. 262.1°C (HPLC-pure) was prepared by recrystallization of the mixture of dicentrine and methanesulfonic acid in equal amounts from MeOH. An analytical HPLC column (Prodigy ODS3 100A, 250 × 4.6 mm, 5 μm; Phenomenex, Torrance, CA) was used in HPLC-SPE-NMR and HPLC-MS. A semipreparative HPLC column (Prodigy ODS3 100A, 250 × 10 mm, 5 μm; Phenomenex) was used for the isolation of metabolites. For the isolated compounds, the ^{1}H NMR and 2D NMR (HMQC or HSQC, HMBC, or NOESY) spectra were measured in an inverse probe of a 600-MHz Avance III NMR spectrometer (Bruker BioSpin, Rheinstetten, Germany), and the ^{13}C NMR spectra were measured either in a QNP probe of a 400-MHz Avance NMR spectrometer (Bruker BioSpin) or in a dual CryoProbe of a 600-MHz Avance III spectrometer. MS data were measured by an Esquire 2000 ion trap mass spectrometer (Bruker Daltonics BioSpin) and a micrOTOF II time-of-flight mass spectrometer with electrospray ion sources (Bruker Daltonics).

Laboratory Animals. Two mature (6 months old) female Langyu small-ear miniature pigs were bred at Taitung Breeding Animal Propagation, Taiwan Livestock Research Institute, Taitung, Taiwan and were transported to the National Taiwan University Veterinary Hospital for the experiment. They were housed in a sheltered outdoor fenced space with good ventilation and allowed forage and water ad libitum throughout the experiment. The animal experiment was conducted according to a protocol approved by the Institutional Animal Care and Use Committee of National Taiwan University [Approval 95 (073)].

Animal Dosing. Two miniature pigs with the respective weights of 18 and 20 kg were starved 15 h before feeding of dicentrine mesylate (51.3 mg/kg, equivalent to 40.0 mg of dicentrine/kg) through a soft plastic gastric tube. Then the pigs were kept in metabolic cages equipped with normal fodder and water. The urine and feces were collected separately and were stored at 4°C before further processing.

Urine Collection and Pretreatment Procedures. The urine of the first pig was collected over a 0- to 24-h period to give approximately 500 ml, which was passed through an Amberlite XAD-2 column and eluted with H_2O (1.5 liters, fraction A-I) first, followed by MeOH (1.5 liters). The MeOH eluant was evaporated under reduced pressure at 40°C to give the MeOH fraction (370 mg, fraction A-II). Fractionation of fraction A-II on a Sephadex LH-20 column (MeOH-H_2O, 7:3) gave three metabolites containing fractions (fraction A-II-1, 7.8 mg; fraction A-II-2, 16.9 mg; and fraction A-II-3, 9.0 mg), monitored by DAD.

The urine of the second pig was collected separately at intervals of 0 to 14.0, 14.0 to 26.0, and 26.0 to 48.0 h. These urine samples were freeze-dried first and then were extracted by 90% $MeOH_{(aq)}$ (two 20-ml extractions). The extracts were evaporated under reduced pressure at 40°C and then were analyzed by HPLC-DAD-MS. The 90% $MeOH_{(aq)}$ urine extract collected at 14 to 26 h (fraction B-I, 9.86 g) was fractionated on a Sephadex LH-20 column (MeOH-H_2O 8:2, o.d. 3.5 cm, height 62 cm) to give a metabolite-containing fraction (fraction B-I-1, 1.26 g).

Feces Collection and Pretreatment Procedures. The feces samples were collected over a 0- to 48-h period. They were suspended in 90% $MeOH_{(aq)}$ (5 ml) in a 15-ml centrifuge tube, vortexed, and centrifuged for 10 min at 3000 rpm. The supernatant was collected. This procedure was repeated three times. The combined supernatants were evaporated under reduced pressure at 40°C to yield a residue (560 mg, fraction C). A portion of this residue (10 mg) was dissolved in MeOH (1.0 ml) and filtered through a 0.45-μm membrane for HPLC-DAD-MS analysis. The HPLC condition used was the same as that for fraction A-II.

Isolation of MI-5 and Dicentrine (1) from Fraction A-II-3. Fraction A-II-3 (three 3.0-mg fractions, 9 mg in 60 μl of MeOH) was chromatographed on a semipreparative RP-HPLC column (Phenomenex) delivered by MeCN-0.1% TFA_{aq}, 5:95 to 40:60 in 55 min, to 60:40 in 15 min, to 100:0 in 1 min (all linear gradient) and 100:0 for 10 min, flow rate 3.3 ml/min, and detection 280 nm. **MI-5** (0.7 mg, t_R 20.53–22.00 min) and **1** (0.2 mg, t_R 32.96–34.86 min) and a fraction (fraction A-II-3A, 5.1 mg) containing other metabolites present in fraction A-II-3 were obtained.

HPLC-SPE-NMR. HPLC-DAD-SPE-NMR (400 MHz) was performed using an Agilent 1100 liquid chromatograph (Agilent, Waldbronn, Germany) equipped with a photodiode array detector (Bruker DAD; Bruker, Rheinstetten, Germany), followed by a Prospekt 2 automated solid-phase extraction unit (Spark Holland, Emmen, Holland), containing 96 HySphere Resin GP cartridges (10 × 2 mm, 10–12 μm), which connected to a 30 μl-inverse NMR probe equipped in a 400-MHz Avance NMR spectrometer. The metabolites with UV absorption similar to that of dicentrine (λ_{max} 280 and 310 nm) were identified by HPLC-DAD analysis and were trapped individually by a resin GP cartridge. Throughout the procedure, described in our previous study (Lee et al., 2007), the ^{1}H NMR spectrum of each trapped compound was obtained.

HPLC Conditions. The HPLC conditions in HPLC-DAD-SPE-NMR for the analytical separation of metabolites in fraction A-II and its subfractions were as follows: Prodigy 100A ODS3 column (250 × 4.6 mm, 5 μm); delivery system (linear gradient): MeCN-0.1% TFA_{aq}, 5:95 to 40:60 in 55 min, to 60:40 in 15 min, to 100:0 in 1 min and 100:0 for 10 min at a flow rate 0.5 ml/min. Samples and amount injected were as follows: fraction A-II 1.0 mg (20 μl of MeOH), two times; fraction A-II-1 1.53 mg (20 μl of MeOH), three times; fraction A-II-2 1.06 mg (20 μl of MeOH), three times; and fraction A-II-3A 1.57 mg (20 μl of MeOH), three times; detection was at 280 nm. For fraction B-I-1, the HPLC conditions were as follows: column, same as above; delivery system (linear gradient), MeCN-0.1% TFA_{aq} 7:93 to 25:75 in 50 min, flow rate 0.5 ml/min, detection at 280 and 310 nm, and amount injected, fraction B-I-1 2.5 mg (20 μl for MeOH), three times.

HPLC-HRESIMS and MS/MS Analysis. An HPLC-ESI ion trap mass spectrometer (Esquire 2000) was used in the beginning to trace the dicentrine metabolites in each HPLC fraction. A small portion (5%) of the HPLC flow (HPLC flow rate 0.5 ml/min) was directed into the mass spectrometer via a splitter (1:20). The temperature at the ESI interface heated capillary was set at 573 K, electrospray voltage was set to 4.5 kV, the nebulizer gas (nitrogen) pressure was set to 23 psi, and a dry nitrogen flow of 8.0 l/min was used. The trap drive was set to 29 to 37 (arbitrary units). The capillary exit voltage was set to 101 to 110 V for the positive ion mode and to −101 to 110 V for the negative ion mode. A specific collision energy (0.5 V) was chosen at each fragmentation step for all of the compounds investigated. The function of smart fragmentation was on (SmartFrag Ampl was 30–200%), and the isolation width was 4 *m/z*. Low-resolution electrospray ionization mass spectrometry and MS/MS data were acquired in both positive and negative modes over a scan range of *m/z* 50 to 1000.

HRESIMS Analysis. Time-of-flight mass spectrometry (micrOTOF II) was used to measure the accurate molecular weight of each metabolite. Both HPLC-HRESIMS and direct infusion of pure compounds were performed. The spectrometer was operated under the following conditions: ESI in positive/negative mode and a mass range of *m/z* 50 to 1000. The ESI source was set to the following conditions: drying gas flow rate 4.0 l/min, drying gas temperature 180°C, nebulizer 0.4 bar, and capillary voltage 4.1 kV.

Isolation of MII-1 and 2 and -5–15 from Fraction B-I-1. Fraction B-I-1 (24.4 mg, 15 times; 366 mg in 1.2 ml of H_2O) was chromatographed on a semipreparative RP-HPLC column delivered by linear gradient of MeCN-0.1% TFA_{aq}, 7:93 to 25:75 in 50 min, flow rate 2.5 ml/min, and detection at 285 nm. Twelve compounds (**MII-1**, 1.9 mg; **MII-2**, 1.8 mg; **MII-5**, 3.1 mg; **MII-6**, 4.9 mg; **MII-7**, 8.6 mg; **MII-9**, 7.5 mg; **MII-10**, 7.0 mg; **MII-11**, 1.8 mg; **MII-12**, 3.5 mg; **MII-13**, 2.0 mg; **MII-14**, 6.2 mg; and **MII-15**, 15.1 mg) together with a fraction containing **MII-8** were yielded. The latter fraction (6.2 mg) was further purified via an isocratic condition, MeCN-0.1% TFA_{aq} 11:89, to give pure **MII-8** (3.3 mg, t_R 42.96 min).

Results

HPLC Analysis of the Phase I Metabolites (MI-1–9). The urine collected from the first miniature pig in 24 h after oral administration of the mesylate salt of dicentrine (**1**) (40 mg/kg) was pretreated and separated into metabolite-containing fractions (fraction A-II and subfractions). RP-HPLC and HPLC-MS analyses of these fractions, using the delivery system MeCN-0.1% TFA_{aq} as indicated under *Materials and Methods*, led to the finding of nine phase I metabolites (**MI-1-9**) (Fig. 1) and the parent compound (**1**) as their TFA salts, for which compound labeling was done according to the elution order observed in the RP-HPLC chromatograms. Compounds characterized from fraction A-II were **MI-4**, t_R 35.51 min; **MI-5**, t_R 36.47 min; **MI-8**, t_R

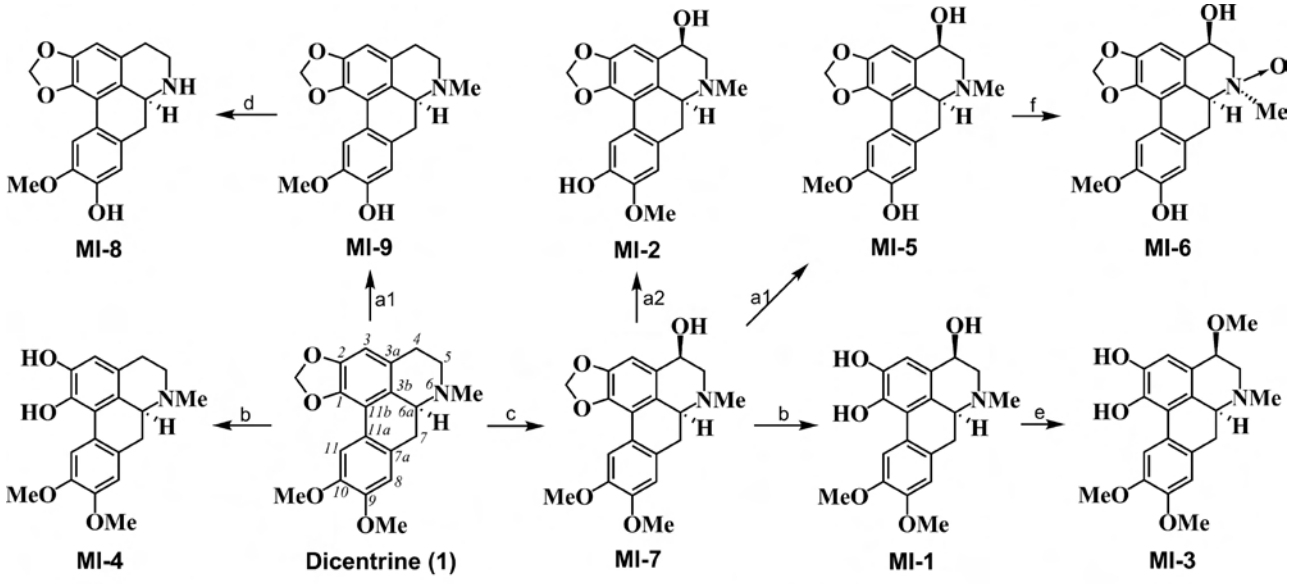

FIG. 1. Proposed phase I metabolic pathways of dicentrine.

42.61 min; **MI-9**, t_R 43.04 min; and **1**, t_R 47.54 min (Fig. 2a; from fraction A-II-1 were **MI-1**, t_R 31.54 min; **MI-6**, t_R 38.31 min; **MI-7**, t_R 41.07 min and **MI-5** (Fig. 2b); from fraction A-II-2 were **MI-3**, t_R 33.94 min; and **MI-1**, **-5**, and **-6**) (Fig. 2c); and from fraction A-II-3A were **MII-2**, t_R 33.84 min; **MI-4**, **-5**, and **-9** (Fig. 2d).

HPLC-SPE-NMR Analysis of the Phase I Metabolites. Dicentrine (**1**) showed characteristic signals for the aromatic H-3, H-8, and H-11 and 1-OCH_2O-2 and the aliphatic H-6a and *N*-Me (Table 1; Supplemental Fig. S1). However, the latter two signals are shifted downfield if the TFA salt is formed (Lee et al., 2007).

Metabolites **MI-4**, **-8**, and **-9** were characterized as the known lastourvilline (*O*,*O*-demethylenyldicentrine) (Eloumi-Ropivia et al., 1985), actinodaphnine (*N*,O^9-didemethyldicentrine) (Lee and Yang, 1992), and cassythicine (*N*-methylactinodaphnine, O^9-demethyldicentrine) (Tewari et al., 1972; Hara et al., 1986), respectively, based on the online ^{1}H NMR (Supplemental Fig. S1 and Table S1) and the $^+$HRESIMS analyses.

Metabolites **MI-1-3** and **-5-7** are all 4β-oxygenated dicentrine derivatives, as exemplified by their ^{1}H NMR spectra (Table 1; Supplemental Fig. S1), all showing a downfield shifted broad singlet with $\delta > 4.30$ ppm, as observed for the H_{eq}-4 in (4*R*,6*aS*)-4-hydroxyaporphines (Hoshino et al., 1975; Yang et al., 1993). The H_{ax}-4 in (4*S*,6*aS*)-4-hydroxyaporphines would appear as a double doublet (J = 6.2, 9.5 Hz) (Hartenstein and Satzinger, 1977). Metabolite **MI-5** had the molecular formula $C_{19}H_{19}NO_5$, as deduced from $^+$HRESIMS showing $[M + H]^+$ at *m/z* 342.1345 (calc. 342.1341), with one oxygen atom more than cassythicine (**MI-9**), suggesting that **MI-5** is 4*R*-hydroxycassythicine. The NOESY spectrum of **MI-5** showing the NOE relationship between H-3 (δ 6.86) and H-4 (δ 4.68, br s), and between H-11 (δ 7.70) and 10-OMe (δ 3.87) (Supplemental Fig. S4) supported this structure elucidation. Metabolite **MI-7** had the molecular formula $C_{20}H_{21}NO_5$, as deduced from $^+$HRESIMS showing $[M + H]^+$ at *m/z* 356.1484 (calc. for $C_{20}H_{21}NO_5$, 356.1498), with an oxygen atom more than dicentrine (**1**), suggesting that it was 4*R*-hydroxydicenrine, a diastereoisomer of the known 4*S*-hydroxydicenrine (Vecchietti et al., 1979). The ^{1}H NMR spectrum of **MI-7**.TFA (Table 1; Supplemental Fig. S1) being almost identical to that of **MI-5**.TFA except for the presence of 9-OMe (δ 3.82) supported this elucidation. Metabolite **MI-2** had the same molecular formula as **MI-5**, as deduced from $^+$HRESIMS. Its ^{1}H NMR spectrum was almost identical to that of **MI-5**, except for a certain shift for H-8 (δ 6.93 versus δ 6.81, **MI-5**) and H-11 (δ 7.58 versus δ 7.70, **MI-5**) (Table 1; Supplemental Fig. S1). Therefore, **MI-2** was reasonably elucidated as 4*R*-hydroxyphanostenine, a structural isomer of **MI-5** with exchanged substitutions at C-9 and C-10. Metabolite **MI-1** had the molecular formula $C_{19}H_{21}NO_5$, as deduced from $^+$HRESIMS showing $[M + H]^+$ at *m/z* 344.1541 (calc. 344.1498), with one oxygen atom more than lastourvilline (**MI-4**). Its ^{1}H NMR spectrum (Table 1; Supplemental Fig. S1) was similar to that of **MI-4**, except for the downfield shifted H-4 (δ 5.02, br s). These data thus established **MI-1** as 4*R*-hydroxylastourvilline. Metabolite **MI-3** had the molecular formula $C_{20}H_{23}NO_5$, as deduced from $^+$HRESIMS showing $[M + H]^+$ at *m/z* 358.1662 (calc. 358.1654), a CH_2 residue more than **MI-1**. Its ^{1}H NMR spectrum was similar to that of **MI-1**.TFA, except for the presence of one additional MeO singlet (δ 3.44) and upfield shifted H-3 and H-4 signals (δ_{H-3} 6.92 versus 6.98 in **MI-1**.TFA; δ_{H-4} 4.36 versus 5.02 in **MI-1**.TFA) (Table 1; Supplemental Fig. S1). The latter shift differences were thus located the methoxy group at C-4 (Nieto et al., 1976). Accordingly, **MI-3** was elucidated as 4*R*-methoxylastourvilline. Metabolite **MI-6** had the molecular formula $C_{19}H_{19}NO_6$, as deduced from $^+$HRESIMS, showing $[M + H]^+$ at *m/z* 358.1299 (calc. 358.1291), with one oxygen atom more than **MI-5**. The ^{1}H NMR spectrum of **MI-6**.TFA (CD_3OD) was similar to that of **MI-5**.TFA except for the downfield shifted signals for H-6a (δ 4.61, dd versus δ 4.05, dd, **MI-5**.TFA) and *N*-Me (δ 3.57 versus δ 3.02, **MI-5**.TFA). The latter two signals (H-6a and *N*-Me), being close to those in boldine N_β-oxide (δ 4.57 and 3.65, respectively) (Lee et al., 2007), thus establishing **MI-6** as an N_β-oxide. Accordingly, the structure of **MI-6** was elucidated as 4*R*-hydroxycassythicine N_β-oxide (Table 1; Supplemental Fig. S1).

For structure confirmation, **MI-5** was further isolated. The unambiguous ^{1}H and ^{13}C NMR assignments for **MI-5** (Table 1) were made by 2D NMR spectral analyses (HMQC and HMBC) (Supplemental Fig. S5).

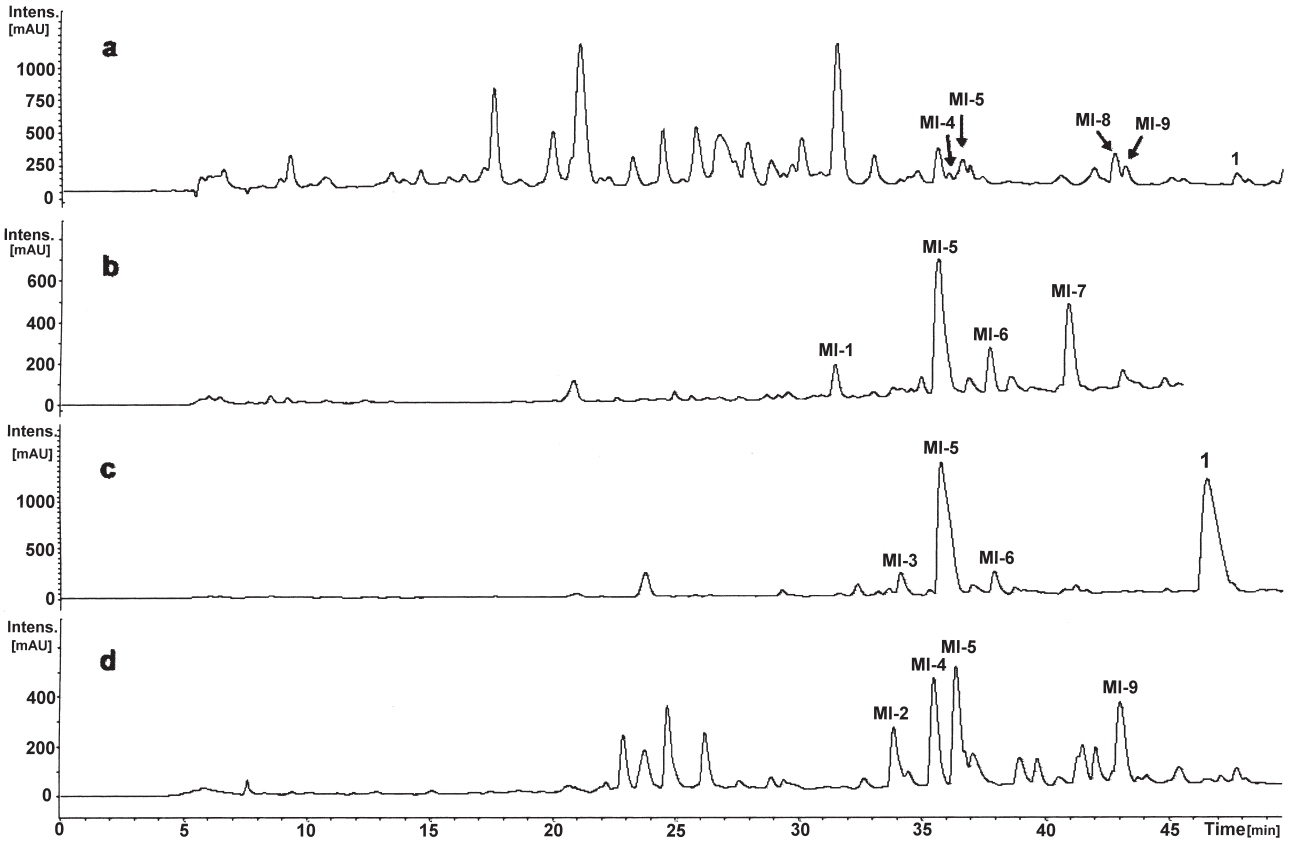

FIG. 2. Reverse-phase HPLC chromatograms of fraction A-II (a), fraction A-II-1 (b), fraction A-II-2 (c), and fraction A-II-3A (d), monitored at UV 280 nm (for other liquid chromatography conditions, see *Materials and Methods*). mAU, milli-absorbance units.

HPLC Analysis of the Phase II Metabolites (MII-1–MII-15). The 90% methanol extract of the urine sample collected at 14.0 to 26.0 h from the second pig was fractionated via Sephadex LH-20 to concentrate the phase II metabolites of dicentrine (**1**) into subfraction fraction B-I-1. HPLC-DAD and HPLC-MS analyses of this fraction, delivered by MeCN-0.1% TFA, led to the finding of 15 metabolites (**MII-1**, t_R 23.80 min; **MII-2**, t_R 25.53 min; **MII-3**, t_R 29.58 min; **MII-4**, t_R 30.79 min; **MII-5**, t_R 31.37 min; **MII-6**, t_R 31.78 min; **MII-7**, t_R 33.92 min; **MII-8**, t_R 35.14 min; **MII-9**, t_R 35.75 min; **MII-10**, t_R 37.19 min; **MII-11**, t_R 39.84 min; **MII-12**, t_R 42.12 min; **MII-13**, t_R 43.83 min; **MII-14**, t_R 45.46 min; and **MII-15**, t_R 45.84 min) (Figs. 3 and 4).

HPLC-SPE-NMR Analysis (MII-3 and -4) and Semipreparative RP-HPLC Separation of the Phase II Metabolites (MII-1 and 2 and -5–15). Following the HPLC analytical conditions for **MII-1–15**, HPLC-SPE-NMR was performed. The online NMR spectra of these compounds are shown in Supplemental Figs. S2 and S3. To confirm the structures of these more sophisticated phase II conjugated metabolites by more extensive 1D and 2D NMR data, most phase II metabolites (**MII-1** and **-2** and **-5–15**) were isolated via semipreparative RP-HPLC, using the delivery system MeCN-0.1% TFA.

Structure Elucidation of the Phase II Metabolites (MII-1–15). The structures of **MII-1–15** were elucidated by ^{1}H and ^{13}C NMR (Tables 2 and 3; Supplemental Tables S2 and S3) and MS (Table 4) data. The molecular formulas of **MII-1–15** are shown in Table 4, as deduced from HRESIMS. From the MS^2 and MS^3 data, **MII-3–15** were identified as monoglucuronide conjugates, whereas **MII-1** was a diglucuronide and **MII-2** was conjugated with one glucuronic acid and one glucose unit (Table 4). The presence of the glucuronyl (GlcUA) group was supported by ^{1}H NMR and correlation spectroscopy data, where GlcUA H-1 appeared as a doublet (J = 7.4–7.8 Hz) around δ 5.00 for 9- or 10-GlcUA (e.g., **MII-3**), around δ 5.30 for 3-GlcUA (e.g., **MII-11** and **-13**), and around δ 4.73 for 1-GlcUA (e.g., **MII-5**), and GlcUA H-5 appeared around δ 3.90 as doublet ($J \approx$ 10 Hz) (Table 2; Supplemental Table S2).

Monoglucuronides. *Metabolites retaining the 1,2-methylenedioxy group (**MII-3 and -9–15**).* **MII-3** and **-9–15** retained a 1,2-methylenedioxy group as verified by the characteristic ^{1}H NMR signals, an AB or AX system around δ 6.00 (Table 2; Supplemental Table S2).

*9-O-Glucuronides (***MII-9**, **-10**, **-14**, and **-15**). The designation of the 9-*O*-GlcUA and 10-OMe in these four metabolites was confirmed by NOESY spectral analysis: H-8 (δ 7.09, **MII-9**; δ 6.98, **MII-10**; δ 7.08, **MII-14**; and δ 6.98, **MII-15**) ↔ 9-*O*-GlcUA H-1 (δ 5.07, **MII-9**; δ 5.20, **MII-10**; δ 5.07, **MII-14**; and δ 5.16, **MII-15**); H-11 (δ 7.68, **MII-9**; δ 7.50, **MII-10**; δ 7.67, **MII-14**; and δ 7.52, **MII-15**) ↔ 10-OMe (δ 3.80, **MII-9**; δ 3.67, **MII-10**; δ 3.81, **MII-14**; and δ 3.64, **MII-15**) (Supplemental Tables S2, S20, S22, S30, and S32). The presence of a 4β-hydroxy group in **MII-9** and **-10** was supported by their ^{1}H NMR data, all of which showed a broad singlet around δ 4.90 in **MII-9** and **-10** (Hoshino et al., 1975), and confirmed by the NOESY spectra, showing the correlation of H-3 (δ 6.86, **MII-9** and δ 6.91, **MII-10**) to H-4α (δ 4.85, **MII-9** and δ 4.92, **MII-10**). In addition, **MII-10** and **MII-15** are *N*-demethylated analogs of **MII-9** and **MII-14**, respectively, based on MS and ^{1}H NMR data. These spectral data thus established them as 4*R*-hydroxycassythicine 9-*O*-β-D-glucuronide (**MII-9**), 4*R*-hydroxyactinodaphnine 9-*O*-β-D-glucuronide (**MII-10**), cassythicine 9-*O*-β-D-glucuronide (**MII-14**), and actinodaphnine 9-*O*-β-D-glucuronide (**MII-15**).

*10-O-Glucuronide **MII-3***. Metabolite **MII-3** had the molecular formula $C_{25}H_{27}NO_{10}$, as deduced from $^+$HRESIMS, being the same as **MII-14** (Table 4). The ^{1}H NMR spectrum of **MII-3**.TFA (Table 2,

DRUG METABOLISM AND DISPOSITION DMD

TABLE 1

*^{1}H NMR data of TFA salts of dicentrine (**1**), **MI-1-3**, and **MI-5-7** from HPLC-SPE-NMR (400 MHz) analysis and ^{13}C NMR and HMBC data for **MI-5***

Position	1	MI-1	MI-2	MI-3	MI-5			MI-6	MI-7
		δ_H^a (J in Hz)			δ_H^b (J in Hz)	HMBC	δ_C^b	δ_H^c (J in Hz)	δ_H^a (J in Hz)
3	6.63 s	6.98 s	6.87 s	6.88 s	6.86 s	1, 2, 4	108.0 d	6.83 s	6.88 s
4		5.02 br s	4.71 br s[d]	4.36 br s[d]	4.68 br s[d]	3a	64.4 t	4.68 br s[d]	4.69 br s[d]
5			3.51 br d (13.1, ax), 3.67 br d (13.1, eq)		3.43 br d (13.0, ax), 3.62 br d (13.0, eq)	3a, 4, 6a	61.0 t		3.44 br d (12.4, ax), 3.63 br d (12.4, eq)
6a			4.14 dd (4.4, 14.2)		4.05 dd (4.4, 13.9)		63.0 d	4.61 dd	4.09 dd (4.6, 13.8)
7			3.02 t (14.2, ax), 3.34 dd (4.4, 14.2, eq)		2.94 t (13.9, ax), 3.28 dd (4.4, 13.9, eq)	3b, 6a, 7a, 8	30.8 t		3.00 t (13.8, ax), 3.34 dd (4.6, 13.8, eq)
8	6.92 s	6.91 s	6.93 s	6.92 s	6.81 s	7, 10, 11a	115.9 d	6.82 s	6.93 s
11	7.70 s	8.04 s	7.58 s	8.06 s	7.70 s	9, 11a	111.4 d	7.70 s	7.70 s
1-OCH_2O-2	6.01 and 6.11 br s		6.05 and 6.14 br s		6.06 and 6.14 br s	1, 2	102.7 t	6.02 and 6.16 br s	6.06 and 6.15 br s
4-OMe				3.44 s					
9-OMe	3.82 s	3.81 s	3.88 s	3.82 s					3.82 s
10-OMe	3.86 s	3.83 s		3.84 s	3.87 s	10	56.7 q	3.87 s	3.84 s
N-Me	2.91 s	2.95 s	3.07 s	3.05 s	3.02 s	5, 6a	42.4 q	3.57 s	3.03 s

ax, axial; eq, equatorial.
[a] Data measured in MeCN-d_3.
[b] ^{1}H and ^{13}CNMR data were obtained from HMQC and HMBC (MeCN-d_3, 600 MHz) analyses, Other ^{13}CNMR data in **MI-5**: δ_C 144.8 (C-1, s), 149.5 (C-2, s), 128.4 (C-3a, s), 121.8 (C-3b, s), 126.8 (C-7a, s), 122.5 (C-11a, s), 116.7 (C-11b, s).
[c] Data measured in MeOH-d_4.
[d] $W_{1/2} \approx 7.0$ Hz.

CD_3OD) adopted from SPE-NMR was similar to that of **MII-14**.TFA except for the shift difference for H-8 (δ 7.03 versus δ 7.08 in **MII-14**.TFA) and H-11 (δ 7.95 versus δ 7.67 in **MII-14**.TFA) (Supplemental Table S2, CD_3OD). Accordingly, **MII-3** is reasonably elucidated as phanostenine 10-*O*-β-D-glucuronide, a structural isomer of **MII-14** with exchanged C-9 and C-10 substitutions.

*Metabolites containing a 3-glucuronyloxy group (**MII-11-13**)*. The ^{1}H NMR spectrum of **MII-11** showed a broad singlet at δ 5.24 but was missing the *N*-Me singlet, suggesting the absence of the *N*-Me group and the presence of a 4β-OH group as stated above (Hoshino et al., 1975). The NOESY spectrum of **MII-11** showed the correlation of H-8/9-OMe and H-11/10-OMe. The HMBC spectrum (Supplemental Fig. S24) showed the correlation of C-3 (δ 137.6, s)/GlcUA H-1 (δ 5.31, d, J = 7.6 Hz), and H-4 (δ 5.24). This structural information incorporated with the MS data thus established **MII-11** as 3-β-D-glucuronyloxy-4*R*-hydroxynordicentrine. **MII-12** had the molecular formula $C_{26}H_{29}NO_{11}$, as deduced from HRESIMS, with one oxygen less than **MII-11**. The ^{1}H NMR spectrum of **MII-12**.TFA (Supplemental Table S2) was similar to that of **MII-11**.TFA (Table 2), except for lacking the downfield shifted H-4 broad singlet, suggesting the absence of the 4β-OH group. These spectral data thus established **MII-12** as 3-β-D-glucuronyloxynordicentrine. This structure was confirmed by the HMBC spectrum (Supplemental Fig. S26), showing the correlation of C-3 (δ 137.3, s)/GlcUA H-1 (δ 5.30, d, J = 7.4 Hz) and H-4s (δ 3.00, m and δ 3.21, dd, J = 5.5, 19.0 Hz). **MII-13** was an *N*-methylated analog of **MII-12**, as evidenced from ^{1}H NMR data (TFA salt), exhibiting an additional *N*-Me at δ 3.17, and MS data, with 14 atomic mass units more than **MII-12**. The assignment of 3-*O*-GlcUA in **MII-13** was confirmed by the correlation of C-3 (δ 136.6, s)/GlcUA H-1 (δ 5.29, d, J = 6.4 Hz) and H-4s (δ 3.07, m and δ 3.26, m) in the HMBC spectrum (Supplemental Fig. S28). Thus, **MII-13** was established as 3-β-D-glucuronyloxydicentrine.

*Metabolites retaining 9,10-dimethoxy groups (**MII-4–8**)*. Metabolites **MII-4–8** are 1,2-*O*,*O*-demethylenated monoglucuronides as indicated by the ^{1}H NMR spectra, lacking the 1-*O*CH_2*O*-2 signals but retaining two methoxy singlets (Table 2; Supplemental Table S2).

*1-O-Glucuronides (**MII-5 and -8**)*. The presence of 1-*O*-GlcUA in **MII-8** (lastourvilline 1-*O*-β-D-glucuronide) was elucidated on the basis of the HMBC spectrum, which showed the correlation of H-3 (δ 6.71) and GlcUA H-1 (δ 4.66)/C-1 (δ 142.4) (Supplemental Fig. S17). The upfield shifted GlcUA H-1 (δ 4.66 versus 5.07, **MII-14**), caused by the anisotropic effect of the bottom ring, also supported the location of this conjugate (Supplemental Table S2). **MII-5** (4*R*-hydroxylastourvilline 1-*O*-β-D-glucuronide) is a 4β-hydroxylated analog of **MII-8**, as exemplified by the MS data and similar ^{1}H NMR data except for the H-4 signals, a broad singlet (δ 4.86) in **MII-5** (Table 2). The NOESY spectrum showing the correlation of H-3/H-4, H-8/9-OMe, and H-11/10-OMe also supported this structure assignment.

*2-O-Glucuronides (**MII-4, -6, and -7**).* **MII-4** (4*R*-hydroxylastourvilline 2-*O*-β-D-glucuronide) had the same molecular formula as **MII-5** (Table 4) and is the structure isomer of **MII-5** with exchanged substituents at C-1 and C-2 as verified by the ^{1}H NMR data. They have similar ^{1}H NMR data except for the downfield shifted H-3 (+0.29 ppm) and H-11 (+0.12 ppm) in **MII-4** relative to the corresponding signals in **MII-5** (Table 2). Likewise, **MII-7** (lastourvilline 2-*O*-β-D-glucuronide) had the same molecular formula as **MII-8** (Table 4) and is the structure isomer of **MII-8** with exchanged substituents at C-1 and C-2 as supported by the similar ^{1}H NMR spectra with difference for the downfield shifted H-3 (+0.28 ppm), H-11 (+0.11 ppm), and GlcUA H-1 (+0.27 ppm) in **MII-7** relative to the corresponding signals in **MII-8** (Supplemental Table S2). The structure for **MII-7** was confirmed by the NOESY spectrum (Supple-

DRUG METABOLISM AND DISPOSITION DMD aspet

TABLE 2

^{1}H NMR data for the TFA salts of metabolites ***MII-1-5***, ***-11***, *and* ***-13***

Position	**MII-1**[a]	**MII-2**[a]	**MII-3**[b]	**MII-4**[b]	**MII-5**[a]	**MII-11**[a]	**MII-13**[a]
	δ_H[a] (*J* in Hz)		δ_H[b] (*J* in Hz)			δ_H[a] (*J* in Hz)	
3	6.68 s	6.69 s	6.68 s	7.20 s	6.91 s		
4	2.99 br d (14.1) 3.28 m	3.01 br d (14.1) 3.27 m	N.D.	4.88 br s	4.86[c] br s ($W_{1/2}$= 6.7 Hz)	5.24 br s ($W_{1/2}$= 6.2 Hz)	3.07 m, 3.26 m
5	3.49 m, 3.77 m	N.D.	N.D.	N.D.	3.68 br d (12.7), 3.62 m	3.64 m, 3.43 m	3.44 m, 3.83 m
6a	4.35 m	N.D.	4.37 br d (15.6)	4.22 br d (13.5)	4.12 br d (12.6)	4.34 m	4.30 br d (15.5)
7	2.85 m, 3.47 m	2.86 m, 3.47 m	N.D.	N.D.	2.90 t (13.8), 2.85 m	3.01 m, 3.07 m	2.83 m 3.44 m
8	7.19 s	7.20 s	7.03 s	6.98 s	6.90 s	6.91 s	6.95 s
11	7.99 s	8.02 s	7.95 s	8.16 s	8.04 s	7.65 s	7.63 s
1-OCH_2O-2	5.94 and 6.10 br s	5.99 and 6.14 br s	5.95 and 6.14 br s			6.08 and 6.16 br s	6.04 and 6.15 br s
9-OMe			3.91 s	3.88 s	3.86 s	3.86 s	3.86 s
10-OMe				3.85 s	3.89 s	3.83 s	3.82 s
N-Me	3.17 s	3.17 s	3.19 s	3.18 s	3.16 s		3.17 s
GlcUA							
1″	5.04 d (7.6)	5.02 d (7.7)	4.94 d (7.8)	N.D.	4.73 d (8.0)	5.31 d (7.6)	5.29 d (6.4)
2′4′	3.49–3.67 m	3.49–3.65 m	3.49–3.67 m	3.49–3.67	3.48–3.67 m	3.50–3.64	3.49 m (2′, 3′), 3.59 m (4′)
5′	3.93 d (10.4)	3.93 d (9.5)	3.96 d (9.7)	3.98 d (10.2)	3.99 d (9.7)	3.88 d (9.5)	3.85 d (9.5)
1‴	4.95 d (7.6)						
5‴	3.94 d (10.4)						
Glc							
1‴		4.90 d (7.7)					
6‴		3.75 dd (5.2, 12.1), 3.85 dd (2.3, 12.1)					

N.D., not detected.

[a] Data were obtained from direct NMR measurement (600 MHz, MeOH-d_4).

[b] Data were obtained from online HPLC-SPE-NMR.

[c] Signals were buried in DOH and were picked up from a 1D selective total correlation spectroscopy experiment.

mental Fig. S15), showing the NOE relationship of GlcUA H-1 (δ 4.93) and H-3 (δ 6.99). **MII-6** (*N*-demethyllastourvilline 2-*O*-β-D-glucuronide) was the *N*-demethylated analog of **MII-7** as evidenced by the MS data (Table 4), the 14 atomic mass units less than **MII-7**, and their similarity in ^{1}H NMR spectra except for a lack of the *N*-Me signal in **MII-6** (Supplemental Table S2).

Di Conjugates. *9,10-Di-O-glucuronide **MII-1***. As described above, **MII-1**, having the molecular formula $C_{30}H_{33}NO_{16}$ as deduced from HRESIMS, contained two GlcUA moieties as elucidated from MS^2 and MS^3 data (Table 4). The ^{1}H NMR spectrum (CD_3OD, 600 MHz) of **MII-1**.TFA (Table 2) showed the signals for 1-OCH_2O-2, three aryl protons, and *N*-Me in the aporphine moiety and two GlcUA H-1 (δ 5.04 and 4.95, each d, J = 7.6 Hz) and GlcUA H-5 (δ 3.94 and 3.93, each d, J = 10.4 Hz) in the glucuronide moieties. These data and the NOESY spectrum (Supplemental Fig. S7) showing the NOE relationship of H-8 (δ 7.19)/9-*O*-GlcUA H-1 (δ 5.04, H′) and H-11 (δ 7.99)/10-*O*-GlcUA H-1 (δ 4.95, H-1″) thus established **MII-1** as *O*-demethylcassythicine 9,10-di-*O*-β-D-glucuronide.

10-O-Glucosyl-9-O-glucuronide **MII-2**. **MII-2** had the molecular formula $C_{30}H_{35}NO_{15}$, as deduced from HRESIMS, and contained one GlcUA and one glucosyl moiety as elucidated from MS^2 and MS^3 data (Table 4). The presence of these two conjugates was shown by the ^{1}H NMR spectrum (TFA salt) (Table 2), displaying two anomeric protons at δ 5.02 (d, J = 7.7 Hz) and δ 4.90 (d, J = 7.7 Hz). The HMQC spectrum (Supplemental Fig. S9), showing a one-bond ^{1}H/^{13}C shift correlation for Glc H-6s/Glc C-6 [δ_H 3.75 (dd) and 3.85 (dd)/δ_C 62.1 (t)], further supported **MII-2** containing the Glc moiety. The NOESY spectrum (Supplemental Fig. S9) showed the NOE relationship of GlcUA H-1 (δ 5.02)/H-8 (δ 7.20) and GlcUA H-5 (δ 3.93, d, J = 9.5 Hz), locating 9-*O*-GlcUA. Accordingly, **MII-2** was established as *O*-demethyl-10-*O*-β-D-glucopyranosyl-cassythicine 9-*O*-β-D-glucuronide.

Among these metabolites identified, six phase I metabolites (**MI-1–3** and **-5–7**) and all of the phase II metabolites (**MII-1–15**) are new chemical entities. The ^{1}H NMR data (Supplemental Table S2) and ^{13}C NMR data (Table 3) of eight metabolites (**MII-6–10**, **-12**, **-14** and **-15**) were assigned based on analysis of 1D and 2D NMR (correlation spectroscopy, NOESY, HSQC, and HMBC) spectra. The ^{13}C NMR data of **MII-1–5**, **-11**, and **-13** and **MI-5** (Supplemental Table S3) were obtained indirectly from the HMBC and HSQC spectral analyses because of limited amounts of materials. The physical data of these metabolites, including UV, specific rotation (isolated ones), circular dichroism, and MS data (**MI-1–9**) are included as Supplemental Data.

The HPLC-DAD analysis of fraction C, obtained from feces, showed no detectable peak having UV absorption similar to dicentrine. Furthermore, attempts to screen the potential sulfate conjugates based on the MS data were made via HPLC-DAD-MS, but none of them were detected in both urine and feces samples.

Discussion

This work led to the characterization of 24 metabolites of dicentrine (**1**) from the urine of miniature pigs, including 9 phase I metabolites (**MI-1–9**) and 15 phase II conjugates (**MII-1–15**). Structural analysis indicates that these phase I metabolites were produced via the generally recognized pathways including C-4 benzylic hydroxylation (**MI-1–3** and **-5–7**), subsequent *O*-methylation (**MI-3**), *N*-oxidation (**MI-7**), *N*-demethylation (**MI-8**), *O*-demethylation (**MI-2**, **-5**, **-6**, **-8**, and **-9**), and *O*,*O*-demethylenation (**MI-1**, **-3**, and **-4**) (Fig. 1).

The amounts of the phase II metabolites were found to be much more than those of the phase I metabolites in the urine, as expected by the facile formation of the glucuronide conjugates to facilitate the

TABLE 3

*^{13}C NMR data for TFA salts of dicentrine (**1**) and metabolites **MII-6–10**, **-12**, **-14**, and **-15***

Position	**1**[a]	**MII-6**[a]	**MII-7**[a]	**MII-8**[b]	**MII-9**[a]	**MII-10**[c]	**MII-12**[a]	**MII-14**[a]	**MII-15**[a]
1	150.1 s	145.0 s	145.0 s	142.4 s	145.8 s	143.5 s	145.8 s	144.6 s	144.3 s
2	144.3 s	147.4 s	147.5 s	152.1 s	150.2 s	148.2 s	138.2 s	150.1 s	149.9 s
3	107.7 d	117.1 d	116.7 d	115.8 d	109.0 d	108.3 d	137.3 s	108.1 d	108.3 d
3a	125.2 s	122.2 s	121.9 s	128.5 s	128.3 s	127.8 s	118.9 s	125.3 s	125.6 s
3b	121.1 s	124.8 s	124.7 s	120.6 s	121.9 s	121.3 s	122.2 s	121.2 s	121.4 s
4	27.1 t	25.9 t	26.7 t	27.0 t	64.4 d	62.0 d	21.9 t	27.1 t	26.4 t
5	54.1 t	42.7 t	54.0 t	53.8 t	60.9 t	48.1 t	42.5 t	54.1 t	42.7 t
6a	63.9 d	54.7 d	64.3 d	64.2 d	63.9 d	52.2 d	54.3 d	63.7 d	54.1 d
7	31.9 t	34.1 t	32.2 t	32.4 t	31.4 t	31.8 t	33.7 t	31.7 t	33.5 t
7a	126.3 s	126.8 s	126.7 s	126.8 s	126.3 s	125.5 s	125.8 s	126.1 s	126.1 s
8	112.9 d	112.5 d	112.6 d	112.2 d	117.1 d	115.2 d	112.9 d	117.5 d	116.3 d
9	150.5 s	149.8 s	149.9 s	150.2 s	147.6 s	146.1 s	150.2 s	147.4 s	146.8 s
10	149.8 s	149.2 s	149.2 s	149.0 s	150.4 s	147.9 s	149.9 s	150.3 s	149.8 s
11	112.1 d	114.4 d	114.3 d	115.9 d	112.9 d	111.6 d	112.2 d	112.9 d	112.8 d
11a	123.9 s	126.0 s	125.8 s	125.4 s	126.0 s	123.7 s	124.2 s	126.1 s	126.1 s
11b	117.6 s	121.7 s	122.0 s	130.0 s	117.1 s	115.0 s	113.2 s	117.3 s	117.0 s
1-OCH_2O-2	102.9 t				103.3 t	101.8 t	103.3 t	103.0 t	102.9 t
9-OMe	56.4 q	56.5 q	56.5 q	56.5 q			56.5 q		
10-OMe	56.6 q	56.6 q	56.6 q	56.6 q	56.9 q	56.1 q	56.7 q	56.8 q	56.6 q
N-Me	42.1 q		42.1 q	42.0 q	42.6 q			42.1 q	
GlcUA									
1′		104.5 d	104.3 d	107.1 d	102.4 d	99.4 d	103.1 d	102.2 d	101.3 d
2′		74.4 d	74.4 d	75.7 d	74.6 d	73.0 d	75.0 d	74.6 d	74.5 d
3′		77.0 d	77.0 d	77.4 d	77.2 d	76.2 d	77.5 d	77.2 d	77.3 d
4′		73.0 d	73.0 d	72.7 d	73.0 d	71.5 d	73.1 d	73.0 d	73.1 d
5′		76.8 d	76.7 d	77.2 d	76.8 d	75.6 d	76.8 d	76.8 d	76.5 d
6′		172.1 s	172.2 s	171.2 s	172.2 s	170.4 s	172.1 s	172.4 s	173.4 s

[a] Measured in MeOH-d_4 (100 MHz).
[b] Measured in MeOH-d_4 (150 MHz).
[c] Measured in dimethyl sulfoxide-d_6 (150 MHz).

TABLE 4

*HRESIMS, ESI-MS, and MS/MS data of **MII-1–15***

Compound	Molecular Formula	HRESIMS			ESIMS		MS^2	
		Parent Ion	*m/z* Observed (Calc.)	Error	Parent Ion	*m/z*	Fragment	*m/z*
				ppm				
MII-1[a]	$C_{30}H_{33}NO_{16}$	$[M+H]^+$	664.1845 (664.1872)	−4.0	$[M-H]^-$	662	$[M-H-GA]^-$	486
MII-2[b]	$C_{30}H_{35}NO_{15}$	$[M+H]^+$	650.2060 (650.2080)	−3.0	$[M-H]^-$	648	$[M-H-GA]^-$	472
MII-3	$C_{25}H_{27}NO_{10}$	$[M+H]^+$	502.1688 (502.1708)	−3.9	$[M-H]^-$	500	$[M-H-GA]^-$	324
MII-4	$C_{25}H_{29}NO_{11}$	$[M+H]^+$	520.1781 (520.1813)	−6.2	$[M-H]^-$	518	$[M-H-GA]^-$	342
MII-5	$C_{25}H_{29}NO_{11}$	$[M-H]^-$	518.1673 (518.1668)	+0.9	$[M-H]^-$	518	$[M-H-GA]^-$	342
MII-6	$C_{24}H_{27}NO_{10}$	$[M+H]^+$	490.1692 (490.1708)	−3.2	$[M+H]^+$	490	$[M+H-GA]^+$	314
MII-7	$C_{25}H_{29}NO_{10}$	$[M-H]^-$	502.1701 (502.1719)	−3.6	$[M+H]^+$	504	$[M+H-GA]^+$	328
MII-8	$C_{25}H_{29}NO_{10}$	$[M-H]^-$	502.1718 (502.1719)	−0.1	$[M+H]^+$	504	$[M+H-GA]^+$	328
MII-9	$C_{25}H_{27}NO_{11}$	$[M-H]^-$	516.1527 (516.1511)	+3.0	$[M-H]^-$	516	$[M-H-GA]^-$	340
MII-10	$C_{24}H_{25}NO_{11}$	$[M-H]^-$	502.1363 (502.1355)	+1.6	$[M-H]^-$	502	$[M-H-GA]^-$	326
MII-11	$C_{25}H_{27}NO_{12}$	$[M+H]^+$	534.1632 (534.1612)	+3.8	$[M-H]^-$	532	$[M-H-GA]^-$	356
MII-12	$C_{25}H_{27}NO_{11}$	$[M-H]^-$	516.1528 (516.1511)	+3.2	$[M-H]^-$	516	$[M-H-GA]^-$	340
MII-13	$C_{26}H_{29}NO_{11}$	$[M-H]^-$	530.1664 (530.1668)	−0.7	$[M+H]^+$	532	$[M+H-GA]^+$	356
MII-14	$C_{25}H_{27}NO_{10}$	$[M+H]^+$	502.1711 (502.1708)	+0.6	$[M+H]^+$	502	$[M+H-GA]^+$	326
MII-15	$C_{24}H_{25}NO_{10}$	$[M-H]^-$	486.1413 (486.1406)	+1.5	$[M-H]^-$	486	$[M-H-GA]^-$	310

[a] MS^3: $[M-H\text{-}2 \times C_6H_8O_6]^-$ at *m/z* 310.
[b] MS^3: $[M-H-C_6H_8O_6-C_6H_{10}O_5]^-$ at *m/z* 310.
[c] GA: $C_6H_8O_6$.

elimination. The major metabolite **MII-15**, as observed from the HPLC-UV chromatogram of fraction B-**I**-1 (Fig. 4), was the 9-*O*-glucuronide of metabolite **MI-8**. It is noted that the phenolic group not only undergoes common glucuronidation but also glucosylation as observed in **MII-2**, similar to that reported for mycophenolic acid (Shipkova et al., 2001). The structures of the metabolites **MII-11–13** also point to the oxidation at the C-3 position in the aryl ring as being one of the phase I transformations (Fig. 3), although the corresponding phase I metabolites were not detected in this study.

Few studies on the metabolism of aporphines had been reported. For example, four phase II metabolites of apomorphine, a drug used in the treatment of Parkinson's disease, had been identified in vitro and in rat urine (Keski-Hynnilä et al., 2002) and also in human urine (van der Geest R et al., 1998). They were characterized as apomorphine 9-*O*-sulfate, 9-*O*-glucuronide, 10-*O*-sulfate, and 10-*O*-glucuronide by HPLC-MS or HPLC-electrochemical detector. Our study revealed the phase II transformation of dicentrine by glucuronidation in miniature pig. No sulfate conjugates were detected in the present study. The in vitro metabolic study of thalicarpine, a dimeric aporphine and benzyltetrahydroisoquinoline alkaloid, indicated three phase I pathways, including *N*-demethylation, aporphine ring oxidation, and benzylic oxidation/reduction (Wu and McKown, 2002). The in vivo metabolic pathways of dicentrine revealed from our study are generally consistent with those observed in thalicarpine and apomor-

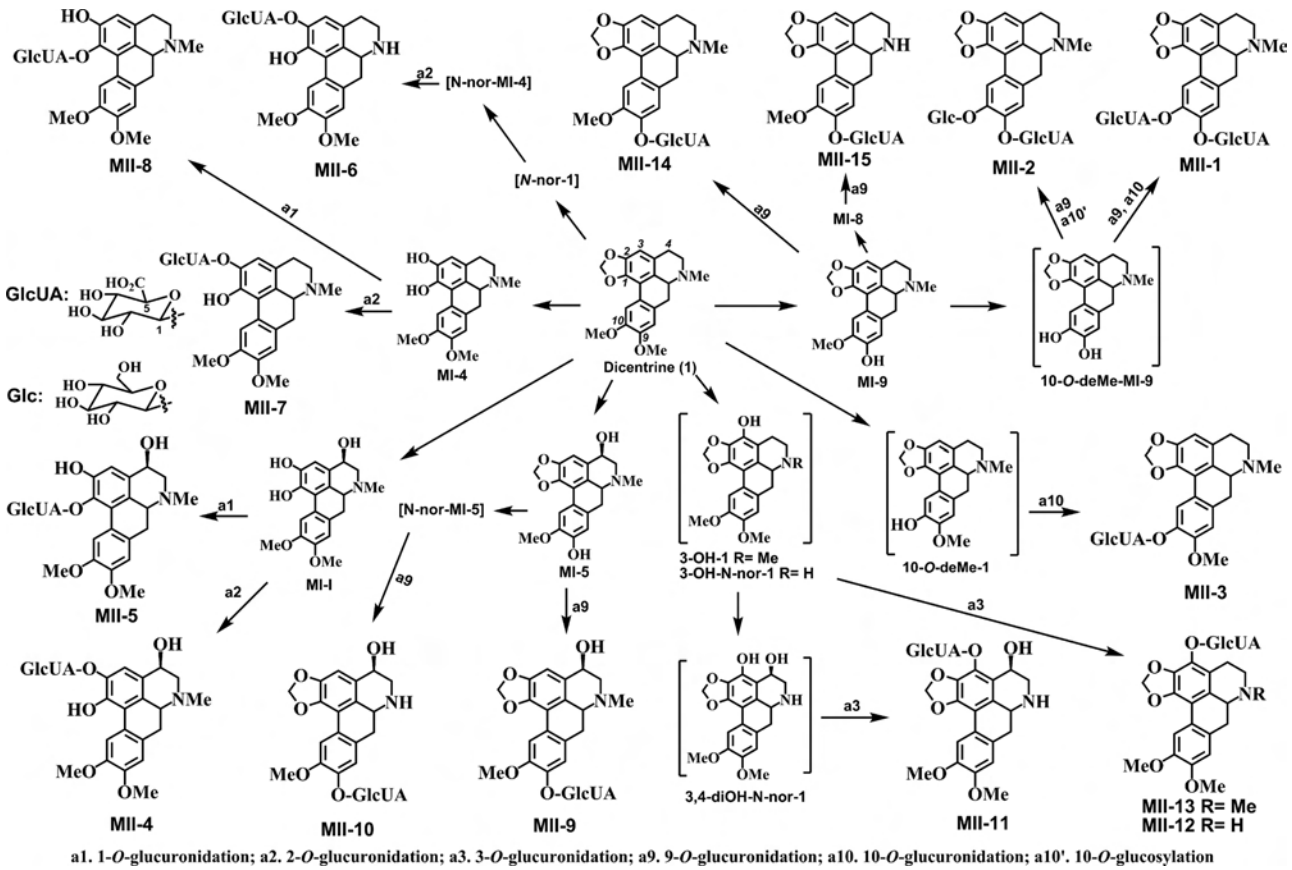

FIG. 3. Proposed phase II metabolic pathways of dicentrine.

phine except for *O*-sulfation, probably attributable to the species difference.

Based on the HPLC-DAD-MS analysis, all of the metabolites identified were from urine, but neither metabolites nor the parent compound were detected from the feces collected during the same period. The result showed that dicentrine mesylate was absorbed well through the gastrointestinal tract and eliminated predominantly through the kidney in the miniature pig.

This study characterized six pairs of structural isomers, including **MI-2/MI-5**, **MI-3/MI-6**, **MII-3/MII-14**, **MII-4/MII-5**, **MII-7/MII-8**, and **MII-9/MII-12**. The structures of these isomeric metabolites were determined by the analysis of MS and informative 1D/2D NMR data. The HPLC-SPE-NMR technique, which requires only submilligram amounts of the desired sample mixture, obtained after appropriate sample pretreatment and focusing, but a baseline resolved HPLC condition, could provide well resolved ^{1}H NMR and ^{1}H-detected 2D NMR spectra for each compound, accelerating greatly for the identification of drug metabolites. Miniature pig, a much larger animal than the commonly used rat, could be administered more samples and therefore provide larger amounts of metabolites, allowing

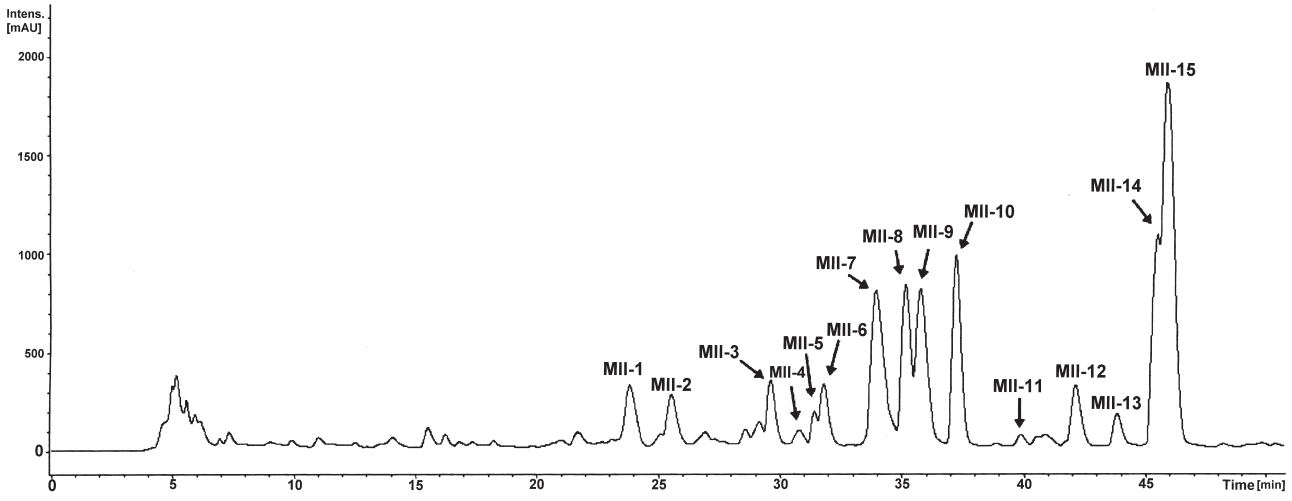

FIG. 4. Reverse-phase HPLC chromatogram of fraction B-I-1, monitored at UV 280 nm (for other liquid chromatography conditions, see *Materials and Methods*). mAU, milli-absorbance units.

their separation in a semipreparative scale and facilitating their unambiguous structural elucidation by general spectroscopic analysis.

These metabolites might be active or toxic. Thus, the preparation of these metabolites would be essential for further clarification of such issue(s) and for exploration of new drug candidates.

Acknowledgments. We thank Dr. C.-C. Chen (National Research Institute of Chinese Medicine, Taipei, Taiwan, Republic of China) for providing dicentrine and W.-C. Su (School of Pharmacy, College of Medicine, National Taiwan University, Taipei, Taiwan, Republic of China) for preparing the dicentrine mesylate salt.

References

Burton KI, Everett JR, Newman MJ, Pullen FS, Richards DS, and Swanson AG (1997) On-line liquid chromatography coupled with high field NMR and mass spectrometry (LC-NMR-MS): a new technique for drug metabolite structure elucidation. *J Pharm Biomed Anal* **15:**1903–1912.

Chang KC, Lo HM, Lin FY, Tseng YZ, Ko FN, and Teng CM (1995) Effects of dicentrine on the mechanical properties of systemic arterial trees in dogs. *J Cardiovasc Pharmacol* **26:**169–176.

Chen CC, Huang YL, Ou JC, Su MJ, Yu SM, and Teng CM (1991) Bioactive principles from the roots of Lindera megaphylla. *Planta Med* **57:**406–408.

De Wet H, Van Heerden FR, Van Wyk BE, and Van Zyl RL (2007) Antiplasmodial activity and cytotoxicity of Albertisia delagoensis. *Fitoterapia* **78:**420–422.

Eloumi-Ropivia J, Beliveau J, and Simon DZ (1985) Isolation of a new alkaloid from Artabotrys lastourvillensis. *J Nat Prod* **48:**460–462.

Godejohann M, Tseng LH, Braumann U, Fuchser J, and Spraul M (2004) Characterization of a paracetamol metabolite using on-line LC-SPE-NMR-MS and a cryogenic NMR probe. *J Chromatogr A* **1058:**191–196.

Hara H, Hashimoto F, Hoshino O, and Umezawa B (1986) Studies on tetrahydroisoquinolines. 28. Syntheses of (±)-*N*-methyllaurotetanine, (±)-cassythicine, (±)-9-hydroxy-1,2,3,10-tetramethoxyaporphine, (±)-dicentrine, and (±)-thalicsimidine. *Chem Pharm Bull* **34:**1946–1949.

Hartenstein J and Satzinger G (1977) Diastereoselective synthesis of the aporphine alkaloid (+)-cataline. Hydroxylation with vanadium (V) trifluoride oxide. *Angew Chem Int Ed Engl* **16:**730–731.

Hoshino O, Hara H, Ogawa M, and Umezawa B (1975) Studies on tetrahydroisoquinolines. X. A stereospecific synthesis of (±)-cataline. *Chem Pharm Bull* **23:**2578–2583.

Israilov IA, Melikov FM, and Muraveva DA (1984) Alkaloids of Dicentra. *Chem Nat Compd* **20:**74–76.

Keski-Hynnilä H, Kurkela M, Elovaara E, Antonio L, Magdalou J, Luukkanen L, Taskinen J, and Kostiainen R (2002) Comparison of electrospray, atmospheric pressure chemical ionization, and atmospheric pressure photoionization in the identification of apomorphine, dobutamine, and entacapone phase II metabolites in biological samples. *Anal Chem* **74:**3449–3457.

Lalezari I, Shafiee A, and Mahjour M (1976) Major alkaloids of Glaucium flavum Grantz, population Ghom. *J Pharm Sci* **65:**923–924.

Lam SH, Wang CY, Chen CK, and Lee SS (2007) Chemical investigation of Phyllanthus reticulatus by HPLC-SPE-NMR and conventional methods. *Phytochem Anal* **18:**251–255.

Lee SS, Lai YC, Chen CK, Tseng LH, and Wang CY (2007) Characterization of isoquinoline alkaloids from Neolitsea sericea var. aurata by HPLC-SPE-NMR. *J Nat Prod* **70:**637–642.

Lee SS and Yang HC (1992) Isoquinoline alkaloids from Neolitsea konishii. *J Chin Chem Soc (Taipei)* **39:**189–194.

Nieto M, Cavé A, and Leboeuf M (1976) Alkaloids of the Annonaceae: composition of the bark of the trunk and roots of Enantia pilosa. *Lloydia* **39:**350–356.

Sandvoss M, Bardsley B, Beck TL, Lee-Smith E, North SE, Moore PJ, Edwards AJ, and Smith RJ (2005) HPLC-SPE-NMR in pharmaceutical development: capabilities and applications. *Magn Reson Chem* **43:**762–770.

Shipkova M, Strassburg CP, Braun F, Streit F, Gröne HJ, Armstrong VW, Tukey RH, Oellerich M, and Wieland E (2001) Glucuronide and glucoside conjugation of mycophenolic acid by human liver, kidney and intestinal microsomes. *Br J Pharmacol* **132:**1027–1034.

Spraul M, Freund AS, Nast RE, Withers RS, Maas WE, and Corcoran O (2003) Advancing NMR sensitivity for LC-NMR-MS using a cryoflow probe: application to the analysis of acetaminophen metabolites in urine. *Anal Chem* **75:**1536–1541.

Stévigny C, Bailly C, and Quetin-Leclercq J (2005) Cytotoxic and antitumor potentialities of aporphinoid alkaloids. *Curr Med Chem AntiCancer Agents* **5:**173–182.

Su MJ, Nieh YC, Huang HW, and Chen CC (1994) Dicentrine, an α-adrenoceptor antagonist with sodium and potassium channel blocking activities. *Naunyn Schmiedebergs Arch Pharmacol* **349:**42–49.

Teng CM, Yu SM, Ko FN, Chen CC, Huang YL, and Huang TF (1991) Dicentrine, a natural vascular alpha 1-adrenoceptor antagonist, isolated from Lindera megaphylla. *Br J Pharmacol* **104:**651–656.

Tewari S, Bhakuni DS, and Dhar MM (1972) Aporphine alkaloids of Litsea glutenosa. *Phytochemistry* **11:**1149–1152.

Tsai TH, Tsai TR, Chou CJ, and Chen CF (1996) Determination of dicentrine in rat plasma by high-performance liquid chromatography and its application to pharmacokinetics. *J Chromatogr B Biomed Appl* **681:**277–281.

van der Geest R, van Laar T, Kruger PP, Gubbens-Stibbe JM, Boddé HE, Roos RA, and Danhof M (1998) Pharmacokinetics, enantiomer interconversion, and metabolism of R-apomorphine in patients with idiopathic Parkinson's disease. *Clin Neuropharmacol* **21:**159–168.

Vecchietti V, Casagrande C, Ferrari G, and Severini Ricca G (1979) New aporphine alkaloids of Ocotea minarum. *Farmaco Sci* **34:**829–840.

Wang CY and Lee SS (2005) Analysis and identification of lignans in Phyllanthus urinaria by HPLC-SPE-NMR. *Phytochem Anal* **16:**120–126.

Wu WN and McKown LA (2002) The in vitro metabolism of thalicarpine, an aporphine-benzyltetrahydroisoquinoline alkaloid, in the rat. API-MS/MS identification of thalicarpine and metabolites. *J Pharm Biomed Anal* **30:**141–150.

Yang MH, Patel AV, Blunden G, Turner CH, O'Neill MJ, and Lewist JA (1993) Crabbine, an aporphine alkaloid from Corydalis lutea. *Phytochemistry* **33:**943–945.

Young ML, Su MJ, Wu MH, and Chen CC (1994) The electrophysiological effects of dicentrine on the conduction system of rabbit heart. *Br J Pharmacol* **113:**69–76.

Yu SM, Chen CC, Ko FN, Huang YL, Huang TF, and Teng CM (1992a) Dicentrine, a novel antiplatelet agent inhibiting thromboxane formation and increasing the cyclic AMP level of rabbit platelets. *Biochem Pharmacol* **43:**323–329.

Yu SM, Hsu SY, Ko FN, Chen CC, Huang YL, Huang TF, and Teng CM (1992b) Haemodynamic effects of dicentrine, a novel alpha 1-adrenoceptor antagonist: comparison with prazosin in spontaneously hypertensive and normotensive Wistar-Kyoto rats. *Br J Pharmacol* **106:**797–801.

Yu SM, Kang YF, Chen CC, and Teng CM (1993) Effects of dicentrine on haemodynamic, plasma lipid, lipoprotein level and vascular reactivity in hyperlipidaemic rats. *Br J Pharmacol* **108:**1055–1061.

Yu SM, Ko FN, Chueh SC, Chen J, Chen SC, Chen CC, and Teng CM (1994) Effects of dicentrine, a novel alpha 1-adrenoceptor antagonist, on human hyperplastic prostates. *Eur J Pharmacol* **252:**29–34.

Address correspondence to: Dr. Shoei-Sheng Lee, School of Pharmacy, College of Medicine, National Taiwan University, 1, Sec. 1, Jen-Ai Rd., Taipei, 10051, Taiwan, R.O.C. E-mail: shoeilee@ntu.edu.tw